Published in final edited form as:
Nat Neurosci. 2014 September ; 17(9): 1198–1207. doi:10.1038/nn.3783.

Cocaine Exposure Reorganizes Cell-Type and Input-Specific Connectivity in the Nucleus Accumbens

Andrew F. MacAskill[1], **John M. Cassel**, and **Adam G. Carter**[*]
Center for Neural Science, New York University, 4 Washington Place, New York, 10003

Abstract

Exposure to cocaine alters the structural and functional properties of medium spiny neurons (MSNs) in the Nucleus Accumbens (NAc). These changes suggest a rewiring of the NAc circuit, with an enhancement of excitatory synaptic connections onto MSNs. However, it is unknown how drug exposure alters the balance of long-range afferents onto different cell types in the NAc. Here we use whole-cell recordings, two-photon microscopy, optogenetics and pharmacogenetics to show how repeated cocaine alters connectivity in the mouse NAc medial shell. We first determine that cocaine selectively enhances amygdala innervation of D1-MSNs relative to D2-MSNs. We then show that amygdala activity is required for cocaine-induced changes to behavior and connectivity. Finally, we establish how heightened amygdala innervation can explain the structural and functional changes induced by cocaine. Our findings reveal how exposure to drugs of abuse fundamentally reorganizes cell-type and input-specific connectivity in the NAc.

Keywords

Cocaine; Nucleus Accumbens; amygdala; hippocampus; medium spiny neuron; two-photon microscopy; optogenetics; pharmacogenetics; spine; synapse

INTRODUCTION

Medium spiny neurons (MSNs) in the Nucleus Accumbens (NAc) play a critical role in the learning and expression of reward-related behaviors[1-3]. Repeated cocaine exposure both induces behavioral sensitization, expressed as heightened locomotion in response to a drug challenge, and alters the synaptic connections onto MSNs[4-10]. After a short withdrawal, cocaine increases the density of dendritic spines on these neurons[11-16], and the frequency of their miniature excitatory postsynaptic currents (mEPSCs)[14]. These structural and functional changes suggest that drug exposure enhances the number of excitatory synapses onto MSNs[8]. However, it remains unknown how repeated cocaine redistributes the connections between different inputs and cell types in the NAc.

[*]Corresponding Author: adam.carter@nyu.edu.
[1]Current address: Department of Neuroscience, Physiology and Pharmacology, University College London, Gower St, London, WC1E 6BT

AUTHOR CONTRIBUTIONS: A.F.M. and A.G.C. designed the experiments. A.F.M. performed the experiments and analyzed the data. J.M.C. performed the stereotaxic injections. A.F.M. and A.G.C. wrote the paper.

The authors have no financial conflicts of interest.

Europe PMC Funders Author Manuscripts

MSNs are segregated into two populations that express either the D1 or D2 subtypes of dopamine receptors[17-19]. D1- and D2-MSNs project to distinct brain regions and play opposing roles in goal-directed and motivated behaviors[20-22]. By reorganizing their excitatory inputs, drug exposure can fundamentally alter how these two cell types are activated. Recent studies indicate that repeated cocaine selectively increases spine density only at D1-MSNs[14,23]. This heightened innervation is thought to promote the activation of these neurons and enable reward-related behaviors[24-26]. However, the types of connections involved in these synaptic rearrangements have not been determined.

Excitatory inputs to the NAc arise from the basolateral amygdala (BLA), ventral hippocampus (VH) and prefrontal cortex (PFC)[27-32]. These long-range afferents carry distinct functional signals and activate MSNs to dictate the output of the NAc[1,2,33]. However, the ability of cocaine to redistribute different types of inputs onto D1- and D2-MSNs is unknown. One possibility is that cocaine-evoked synaptic plasticity involves a subset of afferents and neurons[8]. Interestingly, VH connections are much stronger at D1-MSNs[33], and can be preferentially enhanced by drug exposure[28]. Thus, the observed increase in spine density at D1-MSNs may reflect a selective heightening of VH inputs.

Here we study how repeated cocaine exposure alters cell-type and input-specific connectivity in the NAc medial shell of young adult mice. We first use whole-cell recordings, two-photon microscopy and optogenetics to show that, contrary to our expectations, drug exposure selectively increases BLA inputs onto D1-MSNs. We then use *in vivo* manipulations to demonstrate that BLA activity is required for sensitization and synaptic rearrangements. Finally, we combine these approaches to show how enhanced BLA innervation can explain the increase in spine density and mEPSC frequency at D1-MSNs. Our findings establish how repeated cocaine reorganizes connectivity in the NAc medial shell, highlighting how drug-evoked structural and functional plasticity in this circuit depends on the types of neurons and their afferents.

RESULTS

Cocaine exposure alters synaptic connectivity in the NAc

We investigated how repeated exposure to cocaine alters cell-type and input-specific connectivity in the NAc medial shell of young adult mice. For all experiments, we injected mice with either cocaine (15 mg / kg, i.p.) or control saline once a day for 5 consecutive days[11-16,34] (Fig. 1a). After a short withdrawal, we then assessed either behavioral sensitization or the synaptic properties of MSNs[8]. We first verified that drug exposure induces sensitization by giving a single challenge injection of cocaine (15 mg / kg, i.p.) on day 8. In response to this cocaine challenge, we found that cocaine-treated mice showed enhanced locomotion compared to their saline-treated littermates (saline = 28.7 ± 4.4 m / 10 min; cocaine = 57.9 ± 7.7 m / 10 min; Fig. 1b). Moreover, we found that repeated cocaine progressively enhanced locomotion of mice on successive days (Supplementary Fig. 1). Having established this change in behavior, we then focused on the associated functional and structural changes that occur at D1- and D2-MSNs.

To study how repeated cocaine alters the NAc circuit, we examined the synaptic properties of neighboring D1- and D2-MSNs from cocaine- or saline-treated mice. We directly compared these cell types using hybrid *D1-tdTomato*$^{+/-}$ */ D2-EGFP*$^{+/-}$ mice[35,36] (Fig. 1c). We performed sequential whole-cell recordings from red-only D1-MSNs and green-only D2-MSNs in the same field of view and depth in the slice[33]. We alternated the recording order to avoid any potential bias due to changes in the preparation over time. Finally, in order to directly relate cocaine-induced synaptic and behavioral changes, we performed all recordings on day 8, without any challenge injection of cocaine (Fig. 1a).

We first examined the impact of drug exposure on mEPSCs recorded at −80 mV in the presence of TTX (1 μM) to block action potentials and gabazine (10 μM) to block $GABA_A$ receptors (Fig. 1d). We found that cocaine increased mEPSC frequency only at D1-MSNs (saline: D1 = 1.67 ± 0.23 Hz, D2 = 1.69 ± 0.26 Hz; cocaine: D1 = 2.68 ± 0.35 Hz, D2 = 1.43 ± 0.19 Hz; Fig. 1e). To further compare the two cell types, we also computed the ratio of responses at pairs of neighboring D1- and D2-MSNs (D1/D2 ratio). We found that cocaine caused an increase in the D1/D2 ratio of mEPSC frequency, indicating a bias towards D1-MSNs (D1/D2 ratio: saline = 1.30 ± 0.25, cocaine = 2.73 ± 0.70; Fig. 1e). In contrast, cocaine did not change mEPSC amplitude, which was similar at D1- and D2-MSNs after saline or cocaine (saline: D1 = 20.5 ± 1.4 pA, D2 = 19.9 ± 1.5 pA; cocaine: D1 = 21.0 ± 1.3 pA, D2 = 19.7 ± 1.7 pA; D1/D2 ratio: saline = 1.13 ± 0.12, cocaine = 1.13 ± 0.07; Fig. 1f). These findings indicate that cocaine increases mEPSC frequency at D1-MSNs, which may reflect greater numbers of excitatory inputs[8].

We then assessed whether these functional changes were accompanied by structural alterations at MSNs. We filled neighboring D1- and D2-MSNs with a fluorescent dye (Alexa Fluor 594, 30 μM) via the patch pipette, used two-photon microscopy to image dendritic segments, and generated high-resolution, three-dimensional reconstructions that allowed us to compare spine density (in μm^{-1}) and volume (in μm^3) (Fig. 1g). Consistent with our mEPSC data, we found that cocaine selectively increased spine density only at D1-MSNs (saline: D1 = 1.40 ± 0.09 μm^{-1}, D2 = 1.45 ± 0.09 μm^{-1}; cocaine: D1 = 1.74 ± 0.09 μm^{-1}, D2 = 1.20 ± 0.06 μm^{-1}; D1/D2 ratio: saline = 1.02 ± 0.08, cocaine = 1.47 ± 0.07; Fig. 1h). In contrast, cocaine caused no change in spine volume across all experimental conditions (saline: D1 = 0.42 ± 0.05 μm^3, D2 = 0.34 ± 0.02 μm^3; cocaine: D1 = 0.34 ± 0.03 μm^3, D2 = 0.34 ± 0.02 μm^3; D1/D2 ratio: saline = 1.25 ± 0.14, cocaine = 1.06 ± 0.12; Fig. 1i). These findings indicate that cocaine selectively increases spine density at D1-MSNs, which may reflect greater numbers of excitatory connections[8]. Together, these results confirm that behavioral sensitization is strongly associated with changes to the functional and structural properties of D1-MSNs.

Changes in connectivity are cell-type and input-specific

MSNs in the NAc receive diverse long-range excitatory inputs from the BLA, VH and PFC[27-32]. Cocaine-induced synaptic plasticity could reflect the selective strengthening of a specific input onto D1-MSNs[8]. Alternatively, these changes could reflect a more global enhancement of multiple inputs onto this cell-type[5]. We next explored these possibilities by assessing cocaine-induced changes to cell-type and input-specific connectivity.

To activate long-range excitatory inputs, we used *in vivo* injections of AAV9-CAG-ChR2-mCherry to express Channelrhodopsin-2 (ChR2) in the BLA, VH or PFC. After allowing for expression and axonal transport, we observed prominent labeling of afferents in the NAc medial shell (Fig. 2a,d and Supplementary Fig. 1). To study synaptic responses, we used wide-field illumination to trigger glutamate release from axons containing ChR2, and measured light-evoked excitatory post-synaptic currents (EPSCs) in voltage-clamp recordings from neighboring D1- and D2-MSNs held at −80 mV[33]. As there are no recurrent excitatory connections in the NAc[3], all light-evoked EPSCs must derive from targeted brain regions. Because the absolute amplitude of these EPSCs depends on the number of activated fibers, we focused our analysis on the relative strength at neighboring D1- and D2-MSNs at the same depth and field of view. For BLA inputs, we found that light-evoked EPSCs were similar at D1- and D2-MSNs in saline-treated mice (D1/D2 ratio = 1.46 ± 0.69; Fig. 2b,c). However, cocaine selectively enhanced EPSCs at D1-MSNs compared to D2-MSNs (D1/D2 ratio = 7.61 ± 3.21). These differences in strength were observed at multiple stimulus intensities, suggesting that they are a robust consequence of repeated cocaine (Supplementary Fig. 2). These findings indicate that drug exposure strongly biases BLA inputs towards D1-MSNs in the NAc medial shell.

Interestingly, when we examined VH inputs, we observed the opposite changes to synaptic connectivity. In saline-treated mice, light-evoked EPSCs were larger at D1-MSNs relative to D2-MSNs (D1/D2 ratio = 3.59 ± 1.82; Fig. 2e,f and Supplementary Fig. 2), similar to baseline conditions in the NAc core[33]. However, this preference was no longer apparent in cocaine-treated mice, as EPSCs became equivalent at D1- and D2-MSNs (D1/D2 ratio = 1.01 ± 0.41). These findings reveal that, contrary to our initial expectations, repeated cocaine dampens VH inputs onto D1-MSNs relative to D2-MSNs.

Finally, when we examined PFC inputs, we found smaller light-evoked EPSCs that were unbiased at D1- and D2-MSNs in saline-treated mice (Supplementary Fig. 3), again similar to baseline conditions in the NAc core[33]. Moreover, we found that these EPSCs remained unbiased in cocaine-treated mice. Together, these results indicate that repeated cocaine exposure has unique effects on different long-range afferents onto D1- and D2-MSNs in the NAc medial shell. More broadly, they indicate that cocaine-induced changes to this circuit reflect both cell-type and input-specific synaptic rearrangements.

Alterations in the number and strength of connections

Previous results indicate that cocaine-evoked synaptic plasticity can involve postsynaptic and presynaptic alterations[4,6]. To begin to distinguish between these possibilities, we next recorded light-evoked, input-specific quantal events (qEPSCs) in the presence of extracellular strontium[33] (Fig. 3a-c). This approach provides a direct estimate of postsynaptic efficacy (qEPSC amplitude), and an indirect estimate of the number of connections (qEPSC frequency). As the frequency of qEPSCs depends on the number of activated fibers, we again focused our analysis on the relative values at neighboring D1- and D2-MSNs. In contrast, because the amplitude of qEPSCs depends on receptor properties, we were also able to assess changes across saline and cocaine conditions.

When we examined BLA inputs, we found that qEPSC frequency was initially similar at D1- and D2-MSNs in saline-treated mice (D1 = 5.64 ± 1.32 Hz, D2 = 4.38 ± 0.77 Hz, D1/D2 ratio = 1.15 ± 0.13; Fig. 3d). However, cocaine caused an increase in qEPSC frequency at D1-MSNs compared to D2-MSNs (D1 = 6.27 ± 0.64 Hz, D2 = 3.63 ± 0.75 Hz, D1/D2 ratio = 3.34 ± 1.55). In contrast, the qEPSC amplitude was similar in saline-treated mice, but unaltered by cocaine (saline: D1 = 19.8 ± 2.2 pA, D2 = 19.2 ± 1.5 pA; cocaine: D1 = 24.1 ± 3.2 pA, D2 = 21.1 ± 3.0 pA; D1/D2 ratio: saline = 1.03 ± 0.07, cocaine = 1.23 ± 0.13; Fig. 3e). These findings are consistent with those observed at the whole-cell level, indicating that changes also occur at single synapses. Interestingly, the increased frequency of BLA qEPSCs also mirrors changes to non-specific mEPSCs, suggesting an increase in the number of synapses onto D1-MSNs.

For VH inputs, we found that qEPSC frequency was also similar at D1- and D2-MSNs in saline-treated mice, but unaltered by cocaine (saline: D1 = 5.03 ± 1.08 Hz, D2 = 4.23 ± 1.14 Hz; cocaine: D1 = 7.61 ± 0.96 Hz, D2 = 6.22 ± 1.06 Hz; D1/D2 ratio: saline = 1.35 ± 0.14, cocaine = 1.68 ± 0.66; Fig. 3f). However, the qEPSC amplitude was initially higher at D1-MSNs in saline-treated mice, and this difference was no longer apparent after cocaine, due to a decrease in the amplitude of events on D1-MSNs (saline: D1 = 29.1 ± 2.0 pA, D2 = 17.5 ± 1.4 pA; cocaine: D1 = 22.1 ± 1.9 pA, D2 = 25.3 ± 1.8 pA; D1/D2 ratio: saline = 1.80 ± 0.23, cocaine = 0.87 ± 0.05; Fig. 3g). These results are also consistent with those at the whole-cell level, with smaller VH qEPSCs suggesting postsynaptic effects at D1-MSNs, which are not apparent in the non-specific mEPSCs.

Together, these results suggest that repeated cocaine exposure enhances BLA inputs and suppresses VH inputs onto D1-MSNs. However, the increased frequency of BLA qEPSCs could also be due to increased probability of release. We also examined the paired-pulse ratio (PPR) of BLA and VH EPSCs at neighboring D1- and D2-MSNs, but observed no differences in PPR for either input in saline- and cocaine-treated animals (Supplementary Fig. 4). Therefore, we conclude that the observed changes in the frequency of BLA qEPSCs most likely reflect differences in the number of connections.

Changes in the subcellular properties of connections

Our results suggest that repeated cocaine exposure alters BLA and VH inputs onto MSNs in the NAc medial shell. We next used two-photon mapping to determine if these changes are reflected in the structural properties of these neurons[33,37,38] (Fig. 4a,b). This technique reveals the density and volume of spines contacted by different inputs onto D1- and D2-MSNs. For these experiments, we filled neurons via the patch pipette with a fluorescent dye (Alexa Fluor 594, 30 μM) to image morphology and a calcium indicator (Fluo-4FF, 1 mM) to measure synaptic calcium signals. In voltage-clamp recordings at 0 mV, we isolated dendritic segments containing multiple spines, and triggered presynaptic release from ChR2-containing axons with a pulse of focused blue laser light. We measured light-evoked synaptic calcium signals at spines, which allowed us to detect functional connections, independent of spine volume or distance from the cell body (Supplementary Fig. 5). After sampling dendritic segments at each pair of D1- and D2-MSNs, we generated high-resolution reconstructions of spines and dendrites. We calculated the volume of identified

spines (in μm^3), which provides an indirect measure of postsynaptic efficacy[33,39]. We also determined the number of active spines in each dendritic segment, which provides an estimate of synapse density (in $segment^{-1}$)[38]. As in our physiology experiments, recording from neighboring D1- and D2-MSNs allowed us to assess differences in cell-type and input-specific connectivity.

For BLA inputs, we found that the density of synapses was initially similar at D1- and D2-MSNs in saline-treated mice (D1 = 0.37 ± 0.06 $segment^{-1}$, D2 = 0.57 ± 0.16 $segment^{-1}$, D1/D2 ratio = 0.97 ± 0.27). However, cocaine selectively enhanced synapse density at D1-MSNs compared to neighboring D2-MSNs (D1 = 1.04 ± 0.17 $segment^{-1}$, D2 = 0.44 ± 0.07 $segment^{-1}$, D1/D2 ratio = 2.43 ± 0.35; Fig. 4c). In contrast, there was no difference in spine volume across all four of our experimental conditions (saline: D1 = 0.37 ± 0.13 μm^3, D2 = 0.31 ± 0.08 μm^3; cocaine: D1 = 0.48 ± 0.11 μm^3, D2 = 0.44 ± 0.12 μm^3; D1/D2 ratio: saline = 1.71 ± 0.91, cocaine = 1.52 ± 0.56; Fig. 4d). These findings are consistent with our qEPSC recordings, and together suggest that repeated cocaine selectively enhances the number of BLA connections onto D1-MSNs.

When we examined VH inputs, we observed that synapse density was similar at D1- and D2-MSNs in both saline- and cocaine-treated mice (saline: D1 = 0.96 ± 0.29 $segment^{-1}$, D2 = 0.92 ± 0.27 $segment^{-1}$; cocaine: D1 = 1.12 ± 0.29 $segment^{-1}$, D2 = 1.28 ± 0.20 $segment^{-1}$; D1/D2 ratio: saline = 1.12 ± 0.20, cocaine = 0.88 ± 0.17; Fig. 4e). However, spine volume was initially much larger at D1-MSNs in saline-treated mice, and this difference was abolished after repeated cocaine, due to a reduction in spine volume at D1-MSNs (saline: D1 = 0.65 ± 0.19 μm^3, D2 = 0.21 ± 0.09 μm^3; cocaine: D1 = 0.30 ± 0.14 μm^3, D2 = 0.43 ± 0.06 μm^3; D1/D2 ratio: saline = 5.27 ± 1.79, cocaine = 0.70 ± 0.30; Fig. 4f). These findings are consistent with our qEPSC recordings, and support the idea that drug exposure suppresses the strength of VH connections onto D1-MSNs.

Alterations in connectivity depend on NMDA receptors

Our physiology and imaging results suggest that cocaine reorganizes the NAc circuit in part by enhancing BLA inputs onto D1-MSNs. We next sought to determine if this enhancement can explain the increase in spine density and mEPSC frequency observed at D1-MSNs. NMDA-R activation in the VTA and NAc is critical for the behavioral response to cocaine and associated synaptic plasticity[4,6,40]. Thus, we examined whether activation of NMDA-Rs is also required for the rebalancing of BLA inputs onto D1-MSNs.

We first used *in vivo* pharmacology to test whether NMDA-R activation is required for the induction of behavioral sensitization. We pretreated mice by injecting either the NMDA-R antagonist MK-801 (0.1 mg / kg, i.p.) or control saline 30 min before each cocaine injection on days 1 to 5[34,41] (Fig. 5a). On day 8, we then assessed locomotion in response to a challenge injection of cocaine alone. Consistent with a role for NMDA-Rs in the response to cocaine, we found that MK-801 abolished sensitization (saline = 47.3 ± 6.9 m / 10 min; MK-801 = 29.0 ± 3.1 m / 10 min; Fig. 5b). In control experiments, MK-801 pretreatment had no effect on mice receiving saline instead of cocaine on days 1 to 5 (Supplementary Fig. 6). MK-801 pretreatment also had no effect on baseline locomotion before the cocaine challenge (Supplementary Fig. 6). Finally, acute MK-801 pretreatment before the cocaine

challenge did not prevent subsequent locomotion (Supplementary Fig. 6). These results are consistent with previous studies[40], and confirm that NMDA-R antagonism inhibits the induction of behavioral sensitization.

We then examined whether NMDA-Rs are also required for cocaine-induced synaptic rearrangements. We again pretreated mice with either MK-801 or saline 30 min before each cocaine injection on days 1 to 5. On day 8, we prepared slices and recorded BLA or VH EPSCs from neighboring D1- and D2-MSNs. As in our other physiology experiments, in order to assess cocaine-evoked synaptic plasticity, we did not perform a challenge injection of cocaine. We found that MK-801 pre-treatment blocked cocaine-induced changes to both BLA EPSCs (D1/D2 ratio: saline = 4.76 ± 2.23, MK-801 = 1.13 ± 0.28; Fig. 5c,d) and VH EPSCs (D1/D2 ratio: saline = 0.75 ± 0.16, MK-801 = 5.08 ± 2.74; Fig. 5e,f). These findings indicate that NMDA-Rs are involved in cocaine-induced changes to BLA and VH connections onto MSNs. However, they do not provide a method to dissociate changes to BLA and VH connectivity in the NAc medial shell.

Specific rearrangements depend on amygdala activity

We next used *in vivo* pharmacogenetics to test the roles of afferent brain regions in this cell-type and input-specific synaptic plasticity. We inhibited activity with hM4D, a Designer Receptor Exclusively Activated by Designer Drugs (DREADD) that is activated by the inert agonist clozapine-N-oxide (CNO)[42]. To inhibit neural activity, we used *in vivo* injections of AAV8-CaMKIIa-HA-hM4D-IRES-mCitrine to express hM4D in the BLA, confirming no spread to the VH (Supplementary Fig. 7). After allowing for expression, we recorded from labeled projection neurons in slices, and found that CNO (10 μM) inhibited action potential firing in response to current injections (Supplementary Fig. 7).

We first used this approach to assess whether BLA activity is required for the induction of behavioral sensitization. We bilaterally expressed hM4D in the BLA, and pretreated mice with CNO (0.5 mg / kg, i.p.) 30 min before each cocaine injection on days 1 to 5. On day 8, we then assessed locomotion in response to a challenge injection of cocaine alone (Fig. 6a). Remarkably, we found that inhibiting BLA activity abolished sensitization (control = 60.2 ± 6.8 m / 10 min; hM4D = 33.4 ± 7.8 m / 10 min; Fig. 6b). In control experiments, mice expressing hM4D but pretreated with saline developed normal sensitization (Supplementary Fig. 8). Moreover, CNO pretreatment had no effect on mice receiving saline instead of cocaine on days 1 to 5 (Supplementary Fig. 8). Finally, CNO pretreatment also had no effect on baseline locomotion before the challenge injection of cocaine (Supplementary Fig. 8). Together, these results indicate that BLA activity plays and important role in the induction of behavioral sensitization.

We then tested whether BLA activity is also necessary for cocaine-evoked synaptic plasticity in the NAc medial shell. We performed bilateral injections to express hM4D in the BLA, and unilateral injections to express ChR2 in the BLA (Fig. 6c) or VH (Fig. 6e). We confirmed the selective expression of hM4D in the BLA and ChR2 in the same or different brain regions (Supplementary Fig. 7). After allowing for expression, we pretreated mice with CNO (0.5 mg / kg, i.p.) 30 min before each cocaine injection on days 1 to 5. On day 8, and with no cocaine challenge, we prepared slices and recorded light-evoked EPSCs from

neighboring D1- and D2-MSNs. We found that inhibiting BLA activity abolished cocaine-induced changes to BLA EPSCs (D1/D2 ratio: control = 3.59 ± 1.35, hM4D = 0.89 ± 0.21; Fig. 6d). However, in parallel experiments, inhibiting BLA activity did not block changes to VH EPSCs (D1/D2 ratio: control = 1.25 ± 0.42, hM4D = 1.11 ± 0.34; Fig. 6f). These findings indicate that alterations to BLA and VH EPSCs are dissociable, and that BLA activity is only required for the reorganization of BLA inputs.

In separate experiments, we used equivalent injections to express hM4D bilaterally in the VH (Supplementary Fig. 9), but found that inhibiting VH activity had no significant effect on sensitization (Supplementary Fig. 10). We also used bilateral injections to express hM4D in the VH, and unilateral injections to express ChR2 in the BLA or VH (Supplementary Fig. 9). After treating mice with CNO as described above, we found that inhibiting VH activity had no effect on cocaine-induced changes to BLA EPSCs (Supplementary Fig. 10). However, in parallel experiments, this manipulation abolished changes to VH EPSCs (Supplementary Fig. 10). Together, these findings indicate that VH activity is only required for the reorganization of VH inputs, and confirm that the cocaine-induced rearrangement of BLA connections primarily depends on BLA activity.

Amygdala rearrangements account for enhanced connectivity

Our *in vivo* pharmacogenetics experiments indicate that BLA activity is needed to enhance BLA inputs onto D1-MSNs in the NAc medial shell. We next used this approach to assess whether this enhancement explains the effects of cocaine on mEPSC frequency (Fig. 7). We again performed bilateral injections to express hM4D in the BLA, and pretreated mice with CNO 30 min before each cocaine injection on days 1 to 5. On day 8, and with no cocaine challenge, we prepared slices and recorded mEPSCs at neighboring D1- and D2-MSNs (Fig. 7a). We found that inhibiting BLA activity eliminated the cocaine-induced increase in mEPSC frequency at D1-MSNs (control: D1 = 3.30 ± 0.47 Hz, D2 = 1.74 ± 0.24 Hz; hM4D: D1 = 1.60 ± 0.33 Hz, D2 = 1.84 ± 0.29 Hz; D1/D2 ratio: control = 2.53 ± 0.53, hM4D = 1.27 ± 0.37; Fig. 7b). However, this manipulation had no effect on mEPSC amplitude across all conditions (control: D1 = 21.0 ± 1.0 pA, D2 = 19.5 ± 0.9 pA; hM4D: D1 = 19.8 ± 1.6 pA, D2 = 23.0 ± 2.4 pA; D1/D2 ratio: control = 1.10 ± 0.06, hM4D = 0.96 ± 0.13; Fig. 7c). Because inhibiting BLA activity only prevented changes to BLA EPSCs, these findings indicate that enhanced BLA connectivity can account for the increase in mEPSC frequency.

Finally, we used two-photon imaging to determine whether enhanced BLA innervation also explains the effects of cocaine on spine density (Fig. 7d). We found that inhibiting BLA activity abolished the cocaine-induced increase in spine density at D1-MSNs (control: D1 = 1.81 ± 0.08 μm^{-1}, D2 = 1.05 ± 0.06 μm^{-1}; hM4D: D1 = 1.31 ± 0.09 μm^{-1}, D2 = 1.27 ± 0.05 μm^{-1}; D1/D2 ratio: control = 1.77 ± 0.13, hM4D = 1.03 ± 0.06; Fig. 7e). However, this manipulation had no effect on spine volume across all conditions (control: D1 = 0.36 ± 0.03 μm^3, D2 = 0.48 ± 0.08 μm^3; hM4D: D1 = 0.42 ± 0.06 μm^3, D2 = 0.37 ± 0.03 μm^3; D1/D2 ratio: saline = 0.91 ± 0.20, cocaine = 1.22 ± 0.23; Fig. 7f). These findings indicate that enhanced BLA inputs onto D1-MSNs can also account for the increase in spine density. Together, these results demonstrate that cocaine-evoked structural and functional plasticity reflects heightened BLA innervation of D1-MSNs.

DISCUSSION

We have determined how repeated cocaine exposure reorganizes cell-type and input-specific connectivity in the NAc medial shell of young adult mice. We first used electrophysiology, optogenetics and two-photon microscopy to show that drug exposure selectively heightens BLA inputs onto D1-MSNs. We then used *in vivo* pharmacology and pharmacogenetics to establish that both NMDA-Rs and BLA activity are required for these rearrangements. Finally, we determined that this enhanced BLA innervation of D1-MSNs explains commonly observed cocaine-induced synaptic alterations to this circuit.

Repeated cocaine followed by short withdrawal leads to robust changes in the structural[11-16] and functional[14,43] properties of MSNs in the NAc medial shell. We first found that increases in mEPSC frequency and spine density occur at D1-MSNs, confirming that these changes are cell-type specific[14,44]. We then performed three independent experiments to establish which long-range excitatory inputs are involved in these synaptic changes. Our EPSC experiments show that cocaine bidirectionally redistributes BLA and VH inputs onto D1-MSNs and D2-MSNs. Our qEPSC and two-photon mapping experiments indicate that cocaine increases the number of BLA inputs onto D1-MSNs. These experiments also indicate that cocaine weakens the strength of individual VH connections onto these neurons. Together, these findings underscore how cocaine-evoked synaptic plasticity in the NAc circuit is both cell-type and input-specific.

Several of our physiology and imaging results suggest that drug exposure selectively enhances BLA inputs onto D1-MSNs in the NAc medial shell. We asked if this enhancement could account for the increase in spine density and mEPSC frequency observed at D1-MSNs. Testing this hypothesis is challenging, because optogenetically evoked synaptic responses depend on the number of activated fibers, which in turn depend on the viral infection, slice orientation and light intensity. In many of our experiments, we normalized for these effects using the ratio of responses at neighboring D1- and D2-MSNs. However, it is often difficult to directly compare synaptic responses between animals, including cocaine- and saline-treated mice. Therefore, the greater D1/D2 ratio could reflect either larger responses at D1-MSNs or weaker responses at D2-MSNs. In order to distinguish between these possibilities, we used *in vivo* manipulations to selectively block synaptic plasticity at BLA connections onto MSNs.

Using *in vivo* pharmacology and pharmacogenetics, we found that cocaine-induced changes to BLA innervation depend on NMDA-Rs and BLA activity. Blocking NMDA-Rs during the induction of sensitization prevented changes to both BLA and VH inputs. In contrast, inhibiting BLA activity during repeated cocaine exposure only prevented changes to BLA inputs. This result allowed us to test if enhanced BLA connectivity underlies the increase in mEPSC frequency and spine density. Consistent with our hypothesis, inhibiting BLA activity also blocked increases in spine density and mEPSC frequency at D1-MSNs. Thus, we conclude that these changes are due to a selective increase in BLA innervation of D1-MSNs. In the future, it will be interesting to assess the roles of other brain regions and connections in these cocaine-induced rearrangements.

While we primarily focused on cocaine-evoked synaptic plasticity, our results also have implications for drug-related behavior. Goal-directed and motivated behavior is regulated by the differential activation of D1- and D2-MSNs in both the NAc[22,25,26] and other parts of the striatum[20,21,24]. Repeated cocaine exposure has been hypothesized to enhance D1-MSN activity by increasing the number of excitatory inputs[8,18]. Under baseline conditions, our results suggest that VH inputs are dominant onto these neurons. Drug exposure fundamentally rebalances connectivity, allowing BLA inputs to assume this role. Thus, the driver for motivated behavior may shift from VH inputs carrying contextual signals to BLA inputs relaying more emotional signals[27,28,31,44]. In future studies, it will be important to explore how these connections are reweighted in experimental paradigms that engage varying degrees of contextual, emotional or goal-directed information.

We used an established drug paradigm to alter synaptic connectivity, but it is important to note that neural circuits are constantly changing after drug exposure. Previous studies investigating the impact of repeated cocaine usually fall into one of three categories: 1–3 days withdrawal[11-16,45], 10–14 days withdrawal[28,46], and 40–45 days withdrawal[29,44,47,48]. Each withdrawal time is associated with unique structural and functional alterations at MSNs in the NAc[8]. Consistent with our study, early withdrawal is associated with increases in spine density[11-16,45] and mEPSC frequency[14], as well as changes to excitability[43]. After medium withdrawal, further increases in mEPSC frequency are accompanied by alterations to mEPSC amplitude[46]. Finally, after prolonged withdrawal, there is also an increase in calcium-permeable AMPA receptors[29,44,47,48]. Notably, many of the structural and functional changes observed at early time points are specific to D1-MSNs, and only become apparent when these cell types are distinguished. Our results show that the synaptic rearrangements associated with sensitization are cell-type and input-specific. In the future, similar studies are needed at other withdrawal times to further characterize how drug exposure reorganizes synaptic connectivity in the NAc.

In addition to the withdrawal time, the method of drug administration plays a critical role in determining how cocaine alters neural circuits. We used an established procedure of 5 days of cocaine injections[11-16,34], but related studies have used a single injection[30] or repeated blocks of injections[23,49]. Interestingly, a single injection followed by 7 days withdrawal has been shown to increase the strength of PFC inputs onto D1-MSNs[30]. In other studies, where animals are allowed to self-administer cocaine, there can be dramatically different effects on synaptic structure and function[29,44,47]. For example, the insertion of calcium-permeable AMPA receptors after 45 days of withdrawal only occurs when cocaine is self-administered[48]. Despite these differences, recent results also indicate that the BLA is also necessary for the synaptic changes associated with self-administered cocaine[44]. Thus, reorganization of BLA afferents may be a common consequence of both experimenter- and self-administered cocaine. In future studies, it will be particularly interesting to determine whether cell-type specific changes also occur with cocaine self-administration. For example, a recent study showed unique roles for VH and PFC connections onto D1-MSNs in the NAc in a model of drug relapse[29].

The synaptic and functional changes in response to cocaine also depend on the exact location within the NAc. We focused on synaptic connections in the NAc medial shell,

which recent studies confirm to be intricately involved in the acquisition of drug-related and motivated behaviors[28,31]. This subregion has also been the primary focus of work on cocaine-induced rearrangements at short withdrawal times[11-15]. In contrast, longer withdrawal times are often required in order to see equivalent changes to synaptic connectivity in the NAc core[49]. This subregion receives distinct patterns of innervation, including more prominent inputs from the PFC, and plays different roles in behavior[1,2,32]. In the future, it will be particularly important to assess how different inputs are redistributed between D1- and D2-MSNs in other parts of the NAc and greater striatum.

With these factors in mind, a recent study investigated how repeated cocaine alters inputs to the NAc medial shell after 10–14 days of withdrawal in adult mice[28]. Although this study did not compare D1- and D2-MSNs, it provided a number of important observations. Consistent with our findings, the main inputs to the NAc medial shell were from VH and BLA, with a smaller contribution from PFC. Also consistent with our results, drug exposure triggered changes to VH connections onto MSNs. However, cocaine increased the strength of VH inputs, whereas we observed a weakening at D1-MSNs. Moreover, cocaine did not alter BLA inputs onto MSNs, whereas we observed a strengthening at D1-MSNs. A likely explanation is that additional reorganization occurs between short and long withdrawal from cocaine[8]. Another possibility is age-dependent differences in the roles of BLA and VH inputs to the NAc medial shell. A final consideration is that we compared EPSCs at neighboring D1- and D2-MSNs in the same slices. We did not attempt to compare light-evoked EPSCs between animals, because they strongly depend on the number of activated inputs, as described above. However, we did compare the amplitudes of qEPSCs and the volume of targeted spines, and these results supported our conclusion of weakened VH connections onto D1-MSNs.

Finally, a common feature of many neuropsychiatric and neurodegenerative diseases is the dramatic alteration in spine size and density that is reflective of aberrant synaptic connectivity[50]. Our findings highlight the importance of considering the types of neurons and synapses involved in these alterations. We show that enhanced innervation of BLA inputs onto D1-MSNs in the NAc medial shell helps to explain commonly observed synaptic changes associated with repeated exposure to cocaine. Moreover, we show how these cell-type and input-specific alterations are closely linked to the development of behavioral sensitization. These results reveal how synaptic changes at the level of individual spines help to explain complex responses to drugs of abuse. More generally, they provide a novel perspective on the investigation of how neural circuits throughout the brain are reorganized in diverse neuropsychiatric and neurodegenerative diseases.

ONLINE METHODS

Animals

Young adult mice (postnatal day (P) 29 to 35) of both sexes in a Swiss-Webster background were used for all experiments. Wild-type mice were used for behavioral studies, and hemizygous BAC D1-tdTomato[36] and BAC D2-EGFP[35] mice were used for physiology and imaging studies. The use of hybrid *D1-tdTomato*$^{+/-}$ */ D2-EGFP*$^{+/-}$ mice expressing both fluorescent reporters enabled a direct comparison of D1-MSNs and D2-MSNs in the same

slices[33]. All animals were kept in a temperature and humidity controlled environment with a 12-hour light / dark cycle (lights on at 7 am). Mice were housed in groups of 2 to 5 animals and underwent intraperitoneal (i.p.) injections between 2 pm and 7 pm in their home cage with cocaine (15 mg / kg; Sigma), MK-801 (0.1 mg / kg; Tocris), or clozapine-N-oxide (CNO) (0.5 mg / kg; Sigma), dissolved in 0.9% saline. All experiments followed guidelines established by the New York University animal welfare committee.

Virus injections

Stereotaxic injections were performed on P10 mice, which were anaesthetized with ketamine (40 mg / kg) and xylazine (5 mg / kg) administered intraperitoneally (i.p.). A single incision was made along the midline to reveal the skull before mounting on a stereotaxic apparatus. The head was leveled and injection coordinates determined relative to bregma (Medial / Lateral, Dorsal / Ventral, Rostral / Caudal; BLA: +3.0, −4.8, −1.4, VH: +2.8, −4.6, −3.1, PFC: +0.3, −2.3, +1.7). Long-shaft borosilicate pipettes with a tip diameter of 5 to 10 μm were backfilled with 0.8 μl of AAV9-CAG-hChR2-mCherry (titer = 7×10^{12} GC / ml, UPenn Vector Core), AAV8-CaMKIIa-HA-hM4D-IRES-mCitrine (titer = 4×10^{12} GC / ml, UNC Vector Core), or AAV8-CaMKIIa-EGFP (titer = 4×10^{12} GC / ml, UNC Vector Core). A small hole was created in the skull over the injection site using a fine needle, and ten 14 nl measures of virus were injected over the course of 10 min, for a total volume of approximately 140 nl. The pipette was left in place for an additional 10 min to minimize diffusion and then slowly removed. The wound was sutured and sealed, and mice recovered for ~30 min on a heat pad before returning to their home cage. Expression occurred in the injected brain region for approximately two weeks until preparation of acute slices for physiology experiments. The locations of injection sites were verified before each recording session. For physiology and imaging experiments in Fig. 6, 7 and Supplementary Fig. 10, GFP expression was used as a control for hM4D expression. For behavioral experiments in Fig. 6 and Supplementary Fig. 8 and 10, control mice underwent a sham surgery in which no virus was injected.

Slice preparation

Medium spiny neurons (MSNs) were studied in acute coronal slices of the Nucleus Accumbens (NAc) medial shell. Mice were anaesthetized with a lethal dose of ketamine and xylazine, and perfused intra-cardially with ice-cold external solution containing (in mM): 65 sucrose, 75 NaCl, 25 $NaHCO_3$, 1.25 NaH_2PO_4, 25 glucose, 2.5 KCl, 1 $CaCl_2$, 5 $MgCl_2$, 0.4 Na-ascorbate, and 3 Na-pyruvate, bubbled with 95% O_2 / 5% CO_2. Coronal slices (300 μm thick) were cut in this solution, and then transferred to ACSF containing (in mM): 119 NaCl, 25 $NaHCO_3$, 1.25 NaH_2PO_4, 21 glucose, 2.5 KCl, 2 $CaCl_2$, 1 $MgCl_2$, 0.4 Na-ascorbate, and 3 Na-pyruvate, bubbled with 95% O_2 / 5% CO_2. After 30 min at 35°C, slices were stored for 30 min at 24°C. All experiments were conducted at room temperature (22 – 24°C), with 10 μM D-serine and 10 μM gabazine present to prevent NMDA-R desensitization and block $GABA_A$-Rs, respectively. For two-photon mapping experiments, the ASCF also contained 1 μM TTX, 100 μM 4-AP and 4 mM calcium to block action potentials, increase presynaptic depolarization, and enhance release probability, respectively[33,37,51]. For experiments in Fig. 3, extracellular calcium was replaced with 2 mM strontium. All chemicals were from Sigma or Tocris.

Electrophysiology

Whole-cell recordings were made from red-only D1-MSNs and green-only D2-MSNs, which were identified by their fluorescent cell bodies and targeted with IR-DIC, as previously described[33]. For sequential recordings from D1-MSNs and D2-MSNs, neurons were identified within a single field of view at the same depth. The recording order was alternated to avoid any potential complications that could be associated with rundown. Borosilicate recording pipettes (2 to 3 MΩ) were filled with (in mM): 135 Cs-gluconate, 10 HEPES, 10 Na-phosphocreatine, 4 Mg_2-ATP, and 0.4 NaGTP (290 to 295 mOsm, pH 7.35 with CsOH). The internal solution also contained 10 mM TEA and 2 mM QX-314 to block potassium and sodium channels, respectively. For two-photon mapping experiments, the internal solution also contained 30 μM Alexa Fluor 594 to view morphology and 1 mM Fluo-4FF to monitor calcium. The concentration of Fluo-4FF was chosen to maximize the ability to detect synaptic calcium signals, which were sometimes outside the linear range of the indicator[52]. Neurons were filled via the patch pipette for at least 15 min before commencing imaging. Recordings were made using a Multiclamp 700B amplifier, with electrical signals filtered at 2 kHz and sampled at 10 kHz.

Optogenetics

Presynaptic glutamate release was triggered by illuminating ChR2 in the presynaptic terminals of different long-range excitatory inputs in the NAc, as previously described[33]. For whole-cell experiments, wide-field illumination was achieved with a 1 ms pulse of blue light from an LED centered at 473 nm (ThorLabs). Light intensity was measured as 4 to 7 mW at the back aperture of the objective and was constant between all cell pairs. For experiments in Fig. 2, 3, 5 and 6, light intensity was adjusted for each pair to achieve robust responses, which precluded post-hoc omnibus testing. For two-photon mapping experiments, focused illumination was achieved with a 3 ms pulse of blue light from a 473 nm laser, as previously described[33]. The power of the laser was always set to 3 mW at the back aperture of the objective, which minimized photo-damage while maximizing ChR2 activation. The spot size of the laser was ~30 μm, which allowed for local excitation while avoiding stimulation of areas that were outside the imaging window. For PPR experiments in Supplementary Fig. 4, focused laser illumination was used to activate distant axons, in order to minimize any artifacts caused by direct presynaptic depolarization[38].

Two-photon microscopy

Two-photon imaging, mapping and uncaging was performed with a custom microscope, as previously described[53]. For two-photon imaging, 810 nm light from a Ti:Sapphire laser was used to excite Fluo-4FF (green = G) and Alexa Fluor 594 (red = R). Synaptic calcium signals were quantified as changes in green to red fluorescence (ΔG/R), normalized to maximal green to red fluorescence (G_{sat}/R), giving final measurements in units of ΔG/G_{sat}[52]. Reference frame-scans were taken between each acquisition in order to correct for small spatial drift of the preparation. Baseline fluorescence was monitored and recordings were discarded if any increase was detected, which could indicate photo-damage. At the end of each recording, a high-resolution stack of the entire neuron and sampled dendrites was taken for reconstruction of dendrite and spine morphology.

Two-photon mapping was accomplished by combining two-photon imaging and optogenetics, as previously described[33,37,38]. Within a given dendritic segment, active spines were identified using 8 Hz frame-scans at 12.8 μm × 6.4 μm. Each trial consisted of 7 baseline frame scans before a brief flash of focused 473 nm light, followed by 3 additional frame scans to detect synaptic calcium signals. Synaptic responses were identified online after each of ten trials, using custom software written in MATLAB (MathWorks). For each segment, a high-resolution stack (x = 0.13 μm, y = 0.13 μm, z = 0.2 μm per voxel) of the field of view was acquired for morphological analysis.

For two-photon uncaging, MNI-glutamate was bath applied at 2.5 mM, and glutamate was photo-released using a brief (1 ms) pulse of 725 nm light from a Ti:Sapphire laser to the microscope, as previously described[53]. Uncaging location was at the tip of the spine head, in a line directly perpendicular to the axis of the dendrite. Uncaging was restricted to the top 30 μm of the slice, minimizing any depth effects on the uncaging power.

Spine morphology analysis

High-resolution three-dimensional reconstructions were generated and analyzed using NeuronStudio[13], as previously described[33]. Spine size was quantified as head volume and calculated using a rayburst algorithm[54]. Images were deconvolved prior to head volume measurements using custom routines written in MATLAB (MathWorks).

Histology

Mice were deeply anaesthetized with ketamine and xylazine, as described above. Brains were removed, transferred to a solution containing 4% paraformaldehyde in 0.01 M phosphate-buffered saline (PBS), and fixed for 24 to 48 hours at 4°C. 70 μm coronal sections were prepared using a Leica VT 1000S vibratome, placed on gelatin-coated microscope slides, and sealed under glass coverslips using ProLong Gold antifade reagent with DAPI mounting media (Invitrogen). For immunofluorescence staining, slices were blocked in 1% BSA and 0.4% Triton X-100 in PBS for 1 hr before being incubated overnight at 4°C with an anti-HA antibody (Cell Signaling, C29F4, 1:250) in block solution[55]. Slices were then washed 3 times in PBS and incubated for 1 hour at room temperature in Alexa Fluor 594 or Alexa Fluor 647 conjugated secondary antibody (Molecular Probes) in block solution. Slices were washed 3 times in PBS and then mounted as above. Images were acquired with a Leica SP5 upright confocal microscope using a 40× / 1.25NA oil-immersion objective, or with an Olympus VS120 slide scanner using a 10× / 0.25NA objective. Excitation wavelengths were 405 nm, 488 nm, 561 nm and 633 nm for DAPI, mCitrine, mCherry / Alexa Fluor 594 and Alexa Fluor 647, respectively.

Animal behavior

Behavioral analysis was carried out in a Phenotyper test apparatus (Noldus), which consisted of a 30 cm × 30 cm chamber. All behavioral testing was done between 3pm and 7pm in the light phase of the light cycle. Before testing, mice were handled and habituated to the test apparatus for 2 days. On test day, mice were placed in the test chamber and locomotion was monitored automatically with a digital camera using EthoVision software (Noldus). After 15 minutes habituation to the chamber, mice were given an injection of saline or cocaine (15

mg / kg) and locomotion was then monitored for the 20 minutes immediately after the injection. Analysis was carried out on automatically tracked trajectories calculated using a thresholding method, and plotted as the distance traveled in the 10 minutes immediately after the injection of cocaine.

Data acquisition and analysis

Two-photon imaging and physiology data were acquired using National Instruments boards and custom software written in MATLAB (MathWorks). Offline analysis was performed using custom routines written in Igor Pro (WaveMetrics). The amplitudes of EPSCs are averages over a 2 ms time window around the peak. Identification of mEPSCs and qEPSCs was accomplished using the NeuroMatic plugin for Igor Pro. For this analysis, events were identified within a 50 to 500 ms window after the stimulus, andthe minimal threshold was set to 5 pA.

For each cage, treatment was randomly assigned (e.g., saline vs. cocaine). Where possible, comparisons were made between littermates. In all cases, the experimenter was aware of the conditions being tested, except for the behavioral experiments in Fig. 6 and Supplementary Fig. 8 and 10, in which the experimenter was blind to the manipulation.

Summary data are reported throughout the text and figures as the mean ± SEM. Physiology and imaging data were assessed using a two-way ANOVA followed by Tukey's post-hoc test for multiple comparisons, or a two-sided t-test for paired data. Normality and equal variance were assumed, but not formally tested. Summary comparisons were made using a two-sided Mann-Whitney test, as this is more robust for ratiometric data. Significance was defined as $p < 0.05$ (*). No statistical test was run to determine sample size *a priori*. The sample sizes we chose are similar to those used in previous publications.

Supplementary Material

Refer to Web version on PubMed Central for supplementary material.

Acknowledgments

We thank members of the Carter lab, Mark Farrant and Robert Froemke for helpful discussions and comments on the manuscript, Pamela Kennedy for advice on cocaine administration, and Claudia Farb, Robert Sears and Hannah Seong for help with anatomy. This work was supported by the Dana Foundation, McKnight Foundation and NIH R01DA038138 (AGC). AFM is a Sir Henry Wellcome Postdoctoral Fellow.

REFERENCES

1. Humphries MD, Prescott TJ. The ventral basal ganglia, a selection mechanism at the crossroads of space, strategy, and reward. Progress in Neurobiology. 2010; 90:385–417. [PubMed: 19941931]
2. Sesack SR, Grace AA. Cortico-Basal Ganglia reward network: microcircuitry. Neuropsychopharmacology. 2010; 35:27–47. [PubMed: 19675534]
3. Wilson, CJ. The Synaptic Organization of the Brain. Shepherd, GM., editor. Oxford University Press; 2004.
4. Hyman SE, Malenka RC, Nestler EJ. Neural mechanisms of addiction: the role of reward-related learning and memory. Annual Review of Neuroscience. 2006; 29:565–598.

5. Kalivas PW. The glutamate homeostasis hypothesis of addiction. Nature Reviews. Neuroscience. 2009; 10:561–572.
6. Luscher C, Malenka RC. Drug-evoked synaptic plasticity in addiction: from molecular changes to circuit remodeling. Neuron. 2011; 69:650–663. [PubMed: 21338877]
7. Robinson TE, Kolb B. Structural plasticity associated with exposure to drugs of abuse. Neuropharmacology. 2004; 47(Suppl 1):33–46. [PubMed: 15464124]
8. Russo SJ, et al. The addicted synapse: mechanisms of synaptic and structural plasticity in nucleus accumbens. Trends in Neurosciences. 2010; 33:267–276. [PubMed: 20207024]
9. Schmidt HD, Pierce RC. Cocaine-induced neuroadaptations in glutamate transmission: potential therapeutic targets for craving and addiction. Annals of the New York Academy of Sciences. 2010; 1187:35–75. [PubMed: 20201846]
10. Wolf ME. The Bermuda Triangle of cocaine-induced neuroadaptations. Trends in Neurosciences. 2010; 33:391–398. [PubMed: 20655604]
11. Brown TE, et al. A silent synapse-based mechanism for cocaine-induced locomotor sensitization. The Journal of Neuroscience. 2011; 31:8163–8174. [PubMed: 21632938]
12. Dietz DM, et al. Rac1 is essential in cocaine-induced structural plasticity of nucleus accumbens neurons. Nature Neuroscience. 2012; 15:891–896.
13. Dumitriu D, et al. Subregional, dendritic compartment, and spine subtype specificity in cocaine regulation of dendritic spines in the nucleus accumbens. The Journal of Neuroscience. 2012; 32:6957–6966. [PubMed: 22593064]
14. Kim J, Park BH, Lee JH, Park SK, Kim JH. Cell type-specific alterations in the nucleus accumbens by repeated exposures to cocaine. Biological Psychiatry. 2011; 69:1026–1034. [PubMed: 21377654]
15. LaPlant Q, et al. Dnmt3a regulates emotional behavior and spine plasticity in the nucleus accumbens. Nature Neuroscience. 2010; 13:1137–1143.
16. Maze I, et al. Essential role of the histone methyltransferase G9a in cocaine-induced plasticity. Science. 2010; 327:213–216. [PubMed: 20056891]
17. Gerfen CR, et al. D1 and D2 dopamine receptor-regulated gene expression of striatonigral and striatopallidal neurons. Science. 1990; 250:1429–1432. [PubMed: 2147780]
18. Lobo MK, Nestler EJ. The striatal balancing act in drug addiction: distinct roles of direct and indirect pathway medium spiny neurons. Frontiers in Neuroanatomy. 2011; 5:41. [PubMed: 21811439]
19. Smith Y, Bevan MD, Shink E, Bolam JP. Microcircuitry of the direct and indirect pathways of the basal ganglia. Neuroscience. 1998; 86:353–387. [PubMed: 9881853]
20. Kravitz AV, Tye LD, Kreitzer AC. Distinct roles for direct and indirect pathway striatal neurons in reinforcement. Nature Neuroscience. 2012; 15:816–818.
21. Tai LH, Lee AM, Benavidez N, Bonci A, Wilbrecht L. Transient stimulation of distinct subpopulations of striatal neurons mimics changes in action value. Nature Neuroscience. 2012; 15:1281–1289.
22. Yawata S, Yamaguchi T, Danjo T, Hikida T, Nakanishi S. Pathway-specific control of reward learning and its flexibility via selective dopamine receptors in the nucleus accumbens. Proceedings of the National Academy of Sciences of the United States of America. 2012; 109:12764–12769. [PubMed: 22802650]
23. Lee KW, et al. Cocaine-induced dendritic spine formation in D1 and D2 dopamine receptor-containing medium spiny neurons in nucleus accumbens. Proceedings of the National Academy of Sciences of the United States of America. 2006; 103:3399–3404. [PubMed: 16492766]
24. Ferguson SM, et al. Transient neuronal inhibition reveals opposing roles of indirect and direct pathways in sensitization. Nature Neuroscience. 2011; 14:22–24.
25. Hikida T, Kimura K, Wada N, Funabiki K, Nakanishi S. Distinct roles of synaptic transmission in direct and indirect striatal pathways to reward and aversive behavior. Neuron. 2010; 66:896–907. [PubMed: 20620875]
26. Lobo MK, et al. Cell type-specific loss of BDNF signaling mimics optogenetic control of cocaine reward. Science. 2010; 330:385–390. [PubMed: 20947769]

27. Ambroggi F, Ishikawa A, Fields HL, Nicola SM. Basolateral amygdala neurons facilitate reward-seeking behavior by exciting nucleus accumbens neurons. Neuron. 2008; 59:648–661. [PubMed: 18760700]
28. Britt JP, et al. Synaptic and behavioral profile of multiple glutamatergic inputs to the nucleus accumbens. Neuron. 2012; 76:790–803. [PubMed: 23177963]
29. Pascoli V, et al. Contrasting forms of cocaine-evoked plasticity control components of relapse. Nature. 2014; 509:459–464. [PubMed: 24848058]
30. Pascoli V, Turiault M, Luscher C. Reversal of cocaine-evoked synaptic potentiation resets drug-induced adaptive behaviour. Nature. 2011; 481:71–75. [PubMed: 22158102]
31. Stuber GD, et al. Excitatory transmission from the amygdala to nucleus accumbens facilitates reward seeking. Nature. 2011; 475:377–380. [PubMed: 21716290]
32. Voorn P, Vanderschuren LJ, Groenewegen HJ, Robbins TW, Pennartz CM. Putting a spin on the dorsal-ventral divide of the striatum. Trends in Neurosciences. 2004; 27:468–474. [PubMed: 15271494]
33. MacAskill AF, Little JP, Cassel JM, Carter AG. Subcellular connectivity underlies pathway-specific signaling in the nucleus accumbens. Nature Neuroscience. 2012; 15:1624–1626.
34. Li Y, et al. Both glutamate receptor antagonists and prefrontal cortex lesions prevent induction of cocaine sensitization and associated neuroadaptations. Synapse. 1999; 34:169–180. [PubMed: 10523754]
35. Gong S, et al. A gene expression atlas of the central nervous system based on bacterial artificial chromosomes. Nature. 2003; 425:917–925. [PubMed: 14586460]
36. Shuen JA, Chen M, Gloss B, Calakos N. Drd1a-tdTomato BAC transgenic mice for simultaneous visualization of medium spiny neurons in the direct and indirect pathways of the basal ganglia. The Journal of Neuroscience. 2008; 28:2681–2685. [PubMed: 18337395]
37. Little JP, Carter AG. Subcellular synaptic connectivity of layer 2 pyramidal neurons in the medial prefrontal cortex. The Journal of Neuroscience. 2012; 32:12808–12819. [PubMed: 22973004]
38. Little JP, Carter AG. Synaptic mechanisms underlying strong reciprocal connectivity between the medial prefrontal cortex and basolateral amygdala. The Journal of Neuroscience. 2013; 33:15333–15342. [PubMed: 24068800]
39. Matsuzaki M, et al. Dendritic spine geometry is critical for AMPA receptor expression in hippocampal CA1 pyramidal neurons. Nature Neuroscience. 2001; 4:1086–1092.
40. Wolf ME. The role of excitatory amino acids in behavioral sensitization to psychomotor stimulants. Progress in Neurobiology. 1998; 54:679–720. [PubMed: 9560846]
41. Wolf ME, Jeziorski M. Coadministration of MK-801 with amphetamine, cocaine or morphine prevents rather than transiently masks the development of behavioral sensitization. Brain Research. 1993; 613:291–294. [PubMed: 8186979]
42. Armbruster BN, Li X, Pausch MH, Herlitze S, Roth BL. Evolving the lock to fit the key to create a family of G protein-coupled receptors potently activated by an inert ligand. Proceedings of the National Academy of Sciences of the United States of America. 2007; 104:5163–5168. [PubMed: 17360345]
43. Kourrich S, Thomas MJ. Similar neurons, opposite adaptations: psychostimulant experience differentially alters firing properties in accumbens core versus shell. The Journal of Neuroscience. 2009; 29:12275–12283. [PubMed: 19793986]
44. Lee BR, et al. Maturation of silent synapses in amygdala-accumbens projection contributes to incubation of cocaine craving. Nature Neuroscience. 2013; 16:1644–1651.
45. Huang YH, et al. In vivo cocaine experience generates silent synapses. Neuron. 2009; 63:40–47. [PubMed: 19607791]
46. Kourrich S, Rothwell PE, Klug JR, Thomas MJ. Cocaine experience controls bidirectional synaptic plasticity in the nucleus accumbens. The Journal of Neuroscience. 2007; 27:7921–7928. [PubMed: 17652583]
47. Conrad KL, et al. Formation of accumbens GluR2-lacking AMPA receptors mediates incubation of cocaine craving. Nature. 2008; 454:118–121. [PubMed: 18500330]
48. McCutcheon JE, Wang X, Tseng KY, Wolf ME, Marinelli M. Calcium-permeable AMPA receptors are present in nucleus accumbens synapses after prolonged withdrawal from cocaine

self-administration but not experimenter-administered cocaine. The Journal of Neuroscience. 2011; 31:5737–5743. [PubMed: 21490215]

49. Dobi A, Seabold GK, Christensen CH, Bock R, Alvarez VA. Cocaine-induced plasticity in the nucleus accumbens is cell specific and develops without prolonged withdrawal. The Journal of Neuroscience. 2011; 31:1895–1904. [PubMed: 21289199]
50. Penzes P, Cahill ME, Jones KA, VanLeeuwen JE, Woolfrey KM. Dendritic spine pathology in neuropsychiatric disorders. Nature Neuroscience. 2011; 14:285–293.
51. Petreanu L, Huber D, Sobczyk A, Svoboda K. Channelrhodopsin-2-assisted circuit mapping of long-range callosal projections. Nature Neuroscience. 2007; 10:663–668.
52. Yasuda R, et al. Imaging calcium concentration dynamics in small neuronal compartments. Sci STKE. 2004; 2004:pl5. [PubMed: 14872098]
53. Carter AG, Sabatini BL. State-dependent calcium signaling in dendritic spines of striatal medium spiny neurons. Neuron. 2004; 44:483–493. [PubMed: 15504328]
54. Rodriguez A, Ehlenberger DB, Hof PR, Wearne SL. Rayburst sampling, an algorithm for automated three-dimensional shape analysis from laser scanning microscopy images. Nature Protocols. 2006; 1:2152–2161.
55. Zhu H, et al. Chemogenetic inactivation of ventral hippocampal glutamatergic neurons disrupts consolidation of contextual fear memory. Neuropsychopharmacology. 2014; 39:1880–1892. [PubMed: 24525710]

Europe PMC Funders Author Manuscripts

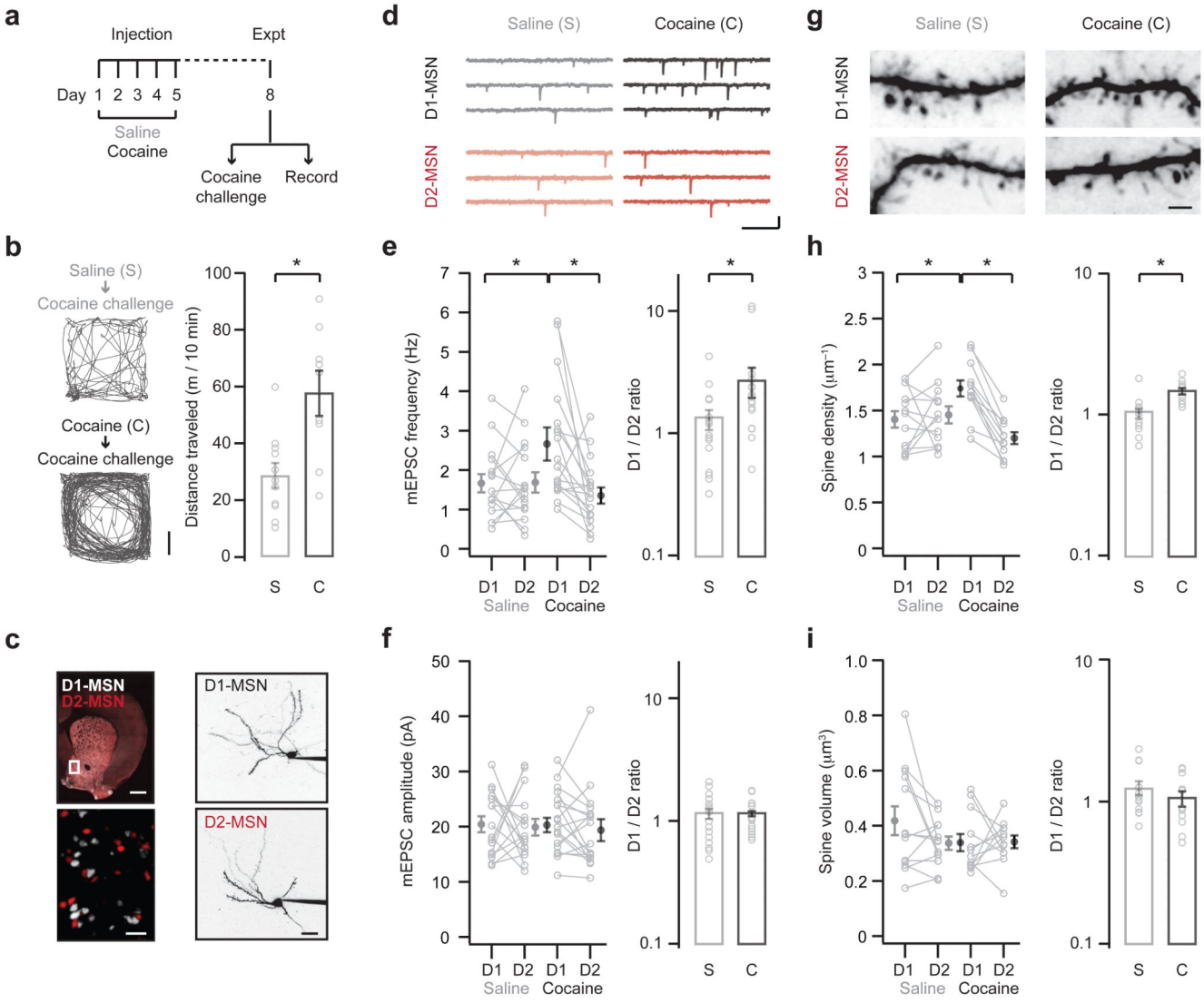

Figure 1. Repeated cocaine enhances excitatory connectivity

a. Schematic of experimental protocol. Cocaine or saline was injected once a day for 5 days. On day 8, animals either received a cocaine challenge to monitor behavioral sensitization (b), or slices were prepared to study the impact on NAc circuitry (c – i). Note that no cocaine challenge was given to animals used for electrophysiology.

b. (Left) Locomotion of saline (top) or cocaine (bottom) mice, measured for 10 min immediately after a cocaine challenge on day 8. Scale bar = 5 cm. (Right) Summary of distance traveled by saline (s) and cocaine (c) mice after the cocaine challenge. Note that mice with previous exposure to cocaine show more pronounced locomotion (U = 14, p = 0.006, Mann-Whitney; n = 11 (s), 9 (c) mice).

c. (Left) Coronal slice from a *D1-tdTomato*$^{+/-}$ / *D2-EGFP*$^{+/-}$ mouse, showing D1- (white) and D2- (red) MSNs. Boxed region in NAc medial shell is magnified. Note the easily identifiable cell bodies. Scale bar = 500 µm. (Right) Two-photon images of D1- (top) and D2- (bottom) MSNs filled via the patch pipette with Alexa Fluor 594. Scale bar = 20 µm.

Europe PMC Funders Author Manuscripts

d. mEPSCs at neighboring D1- (top) and D2- (bottom) MSNs from mice treated with saline (left) or cocaine (right). Scale bars = 10 pA, 200 ms.

e. Summary of mEPSC frequency at D1- and D2-MSNs from saline (s) and cocaine (c) mice. Raw data is shown on the left, and the ratio of mEPSC frequency at pairs of neighboring D1- and D2-MSNs is shown on the right. Note that ratios are plotted on a log axis. Cocaine increases the frequency of mEPSCs at D1-MSNs, thereby increasing the D1/D2 ratio (interaction between drug and cell-type, $F_{(1,64)} = 5.7$, $p = 0.02$, two-way ANOVA; D1-cocaine $p < 0.05$ compared to D1-saline and D2-cocaine, Tukey's post-hoc test; D1/D2 ratio: $U = 75$, $p = 0.02$, Mann-Whitney; n = 16 (s), 18 (c) pairs).

f. Summary of mEPSC amplitude at D1- and D2-MSNs from saline (s) and cocaine (c) mice. Note that cocaine does not alter the amplitude of mEPSCs at D1- or D2-MSNs (no significant effects, two-way ANOVA; D1/D2 ratio: $U = 133$, $p = 0.72$, Mann-Whitney).

g. Two-photon images of dendrites and spines at D1- (top) and D2- (bottom) MSNs from saline (left) or cocaine (right) mice. Scale bar = 2 μm.

h. Summary of spine density at D1- and D2-MSNs in saline (s) and cocaine (c) mice. Raw data is shown on the left, while the ratio of spine density at pairs of neighboring D1- and D2-MSNs is shown on the right. Cocaine increases the spine density at D1-MSNs, thereby increasing the D1/D2 ratio (interaction between drug and cell type, $F_{(1,46)} = 12.1$, $p = 0.001$, two-way ANOVA; D1-cocaine $p < 0.05$ compared to D1-saline and D2-cocaine, Tukey's post-hoc test; D1/D2 ratio: $U = 14$, $p < 0.001$, Mann-Whitney; n = 13 (s), 12 (c) pairs).

i. Summary of spine volume at D1- and D2-MSNs in saline (s) and cocaine (c) mice. Note that cocaine does not alter the spine volume at D1- or D2-MSNs (no significant effects, two-way ANOVA; D1/D2 ratio: $U = 58$, $p = 0.29$, Mann-Whitney).

Bar graphs show mean ± SEM. * denotes $p < 0.05$.

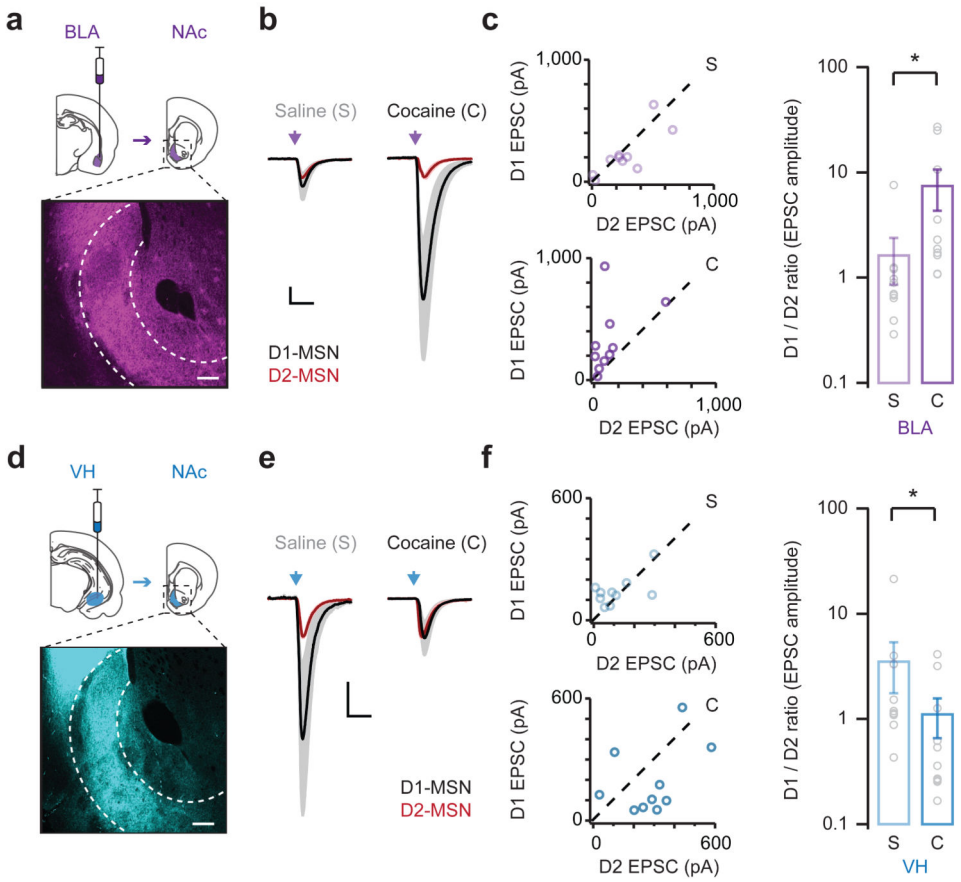

Figure 2. Synaptic plasticity is cell-type and input-specific

a. (Top) Schematic of AAV9-CAG-hChR2-mCherry injection into the basolateral amygdala (BLA, purple) and projection to the NAc. (Bottom) Coronal section of the NAc medial shell (dotted outline), showing distribution of BLA afferents. Scale bar = 100 μm.

b. Light-evoked BLA EPSCs at D1-MSNs (mean in black, error in grey) and D2-MSNs (mean in red, error in pink) on day 8 from animals injected with saline (left) or cocaine (right) on days 1 to 5. EPSCs at D1-MSNs are scaled to those at neighboring D2-MSNs. Scale bar = unity, 20 ms.

c. (Left) Summary of BLA EPSCs at D1- and D2-MSNs in saline (top) and cocaine (bottom) mice. (Right) Summary of D1/D2 ratio of BLA EPSCs. Note that cocaine biases BLA EPSCs towards D1-MSNs, thereby increasing the D1/D2 ratio (D1/D2 ratio: $U = 11$, p = 0.002, Mann-Whitney; n = 10 (s), 10 (c) pairs).

d – f. Similar to (a – c) for ventral hippocampus inputs (VH, blue). Note that cocaine normalizes VH EPSCs at D1- and D2-MSNs, thereby reducing the D1/D2 ratio (D1/D2 ratio: $U = 25$, p 0.02, Mann-Whitney; n = 11 (s), 11 (c) pairs).

Bar graphs show mean ± SEM. * denotes $p < 0.05$.

Europe PMC Funders Author Manuscripts

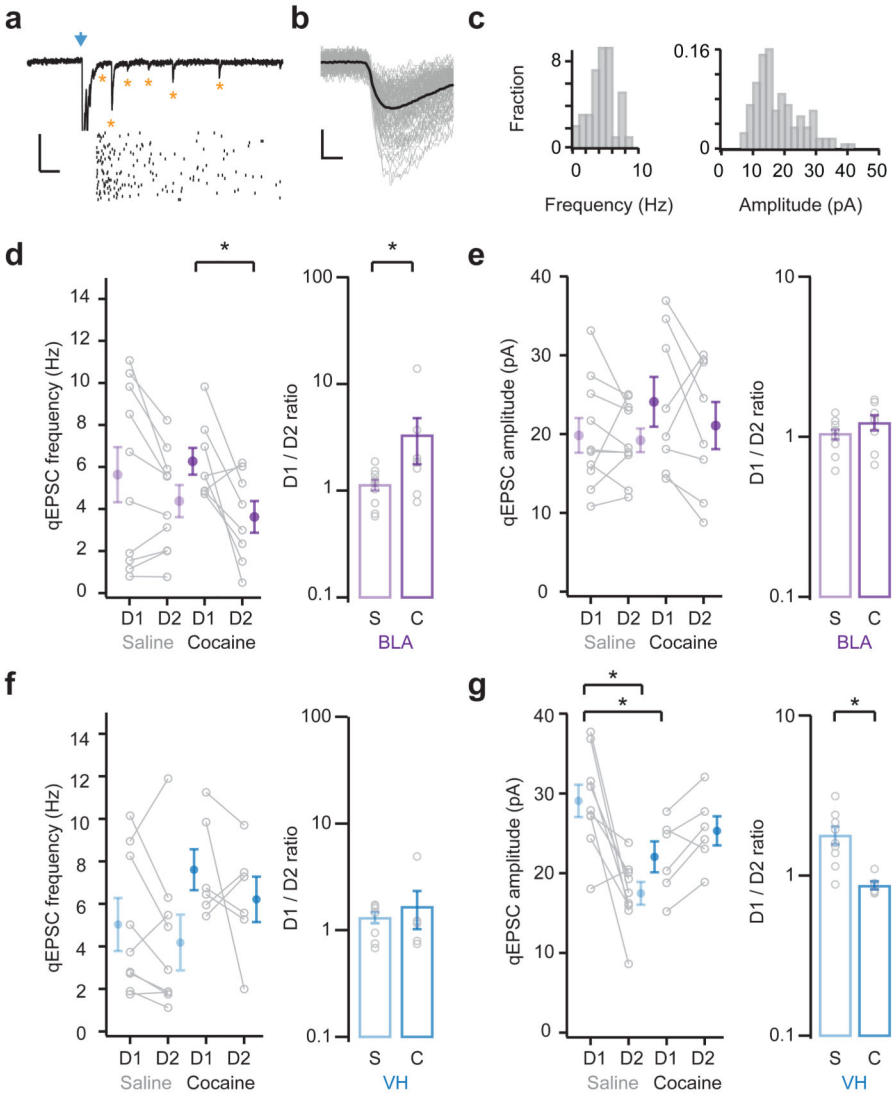

Figure 3. Changes to the number and strength of connections

a. (Top) Light-evoked basolateral amygdala (BLA) qEPSCs recorded in the presence of strontium. Blue arrow indicates light pulse. Asterisks indicate qEPSCs. (Bottom) Raster plot showing qEPSCs detected on individual trials. Scale bar = 30 pA, 100 ms.

b. Overlay of individual (grey) and average (black) onset-aligned qEPSCs from example in (**a**). Scale bar = 10 pA, 2 ms.

c. Histogram of qEPSC frequency (left) and amplitude (right) from example in (**a**).

d. (Left) Summary of the frequency of BLA qEPSCs at D1- and D2-MSNs in saline (s) or cocaine (c) mice. (Right) Summary of D1/D2 ratio of BLA qEPSC frequency. Note that cocaine increases BLA qEPSC frequency at D1-MSNs ($t_{(7)}$ = 2.9, p = 0.02, paired t-test; D1/D2 ratio: U = 16, p = 0.03, Mann-Whitney; n = 10 (s), 8 (c) pairs).

e. (Left) Summary of the amplitude of BLA qEPSCs at D1- and D2-MSNs in saline (s) or cocaine (c) mice. (Right) Summary of D1/D2 ratio of BLA qEPSC amplitude. Note that cocaine has no effect on BLA qEPSC amplitude (no significant effects, two-way ANOVA; D1/D2 ratio: U = 25, p = 0.2, Mann-Whitney).

f, g. Similar to (d, e) for ventral hippocampus inputs (VH). Note that cocaine has no impact on the frequency of VH qEPSCs (D1/D2 ratio: $U = 21$, $p = 0.53$, Mann-Whitney; n = 9 (s), 6 (c) pairs), but reduces their amplitude at D1-MSNs (interaction between drug and cell type, $F_{(1,26)} = 162.7$, $p < 0.001$; D1-saline $p < 0.05$ compared to D1-cocaine and D2-saline, Tukey's post-hoc test; D1/D2 ratio: $U = 2$, $p = 0.002$, Mann-Whitney).
Bar graphs show mean ± SEM. * denotes $p < 0.05$.

Europe PMC Funders Author Manuscripts

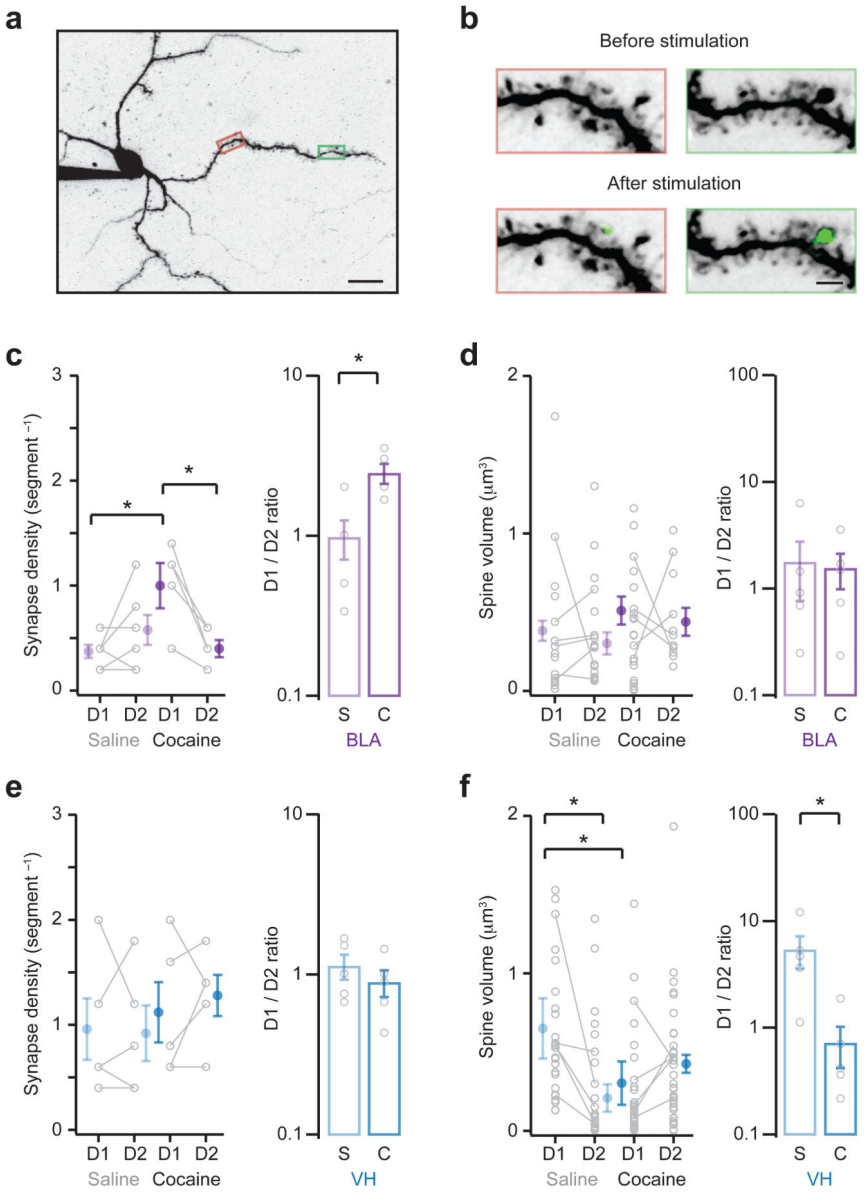

Figure 4. Alterations to structural connections at dendritic spines

a. Two-photon image of MSN filled with Alexa Fluor 594 and Fluo-4FF via the patch pipette, showing dendrites and spines.

b. Boxed areas in (a) are enlarged to show before (top) and after (bottom) light stimulation of ChR2-expressing VH inputs. Synaptic connections are detected by calcium signals (green) at individual dendritic spines. Scale bars = 20 µm and 2 µm.

c. (Left) Summary of density of BLA synapses at D1- and D2-MSNs in saline (s) or cocaine (c) mice. (Right) Summary of D1/D2 ratio of BLA synapse density. Cocaine increases BLA synapse density at D1-MSNs (interaction between drug and cell type, $F_{(1,18)} = 10.0$, p = 0.005, two-way ANOVA; D1-cocaine p < 0.05 compared to D1-saline and D2-cocaine, Tukey's post-hoc test; D1/D1ratio: $U = 2$, p = 0.02, Mann-Whitney; n = 6 (s), 5(c) pairs).

d. (Left) Summary of volume of spines contacted by BLA inputs at D1- and D2-MSNs in saline (s) or cocaine (c) mice. (Right) Summary of D1/D2 ratio of BLA spine volume. Note that cocaine does not alter BLA spine volume (no significant effects, two-way ANOVA; D1/D2 ratio: $U = 13$, $p = 0.79$, Mann-Whitney).

e, f. Similar to (c, d) for VH inputs. Note that cocaine has no effect on VH synapse density (no significant effects, two-way ANOVA; D1/D2 ratio: $U = 8$, $p = 0.41$, Mann-Whitney; n = 5 (s), 5 (c) pairs), but decreases VH spine volume at D1-MSNs (interaction between drug and cell type, $F_{(1,99)} = 11.1$, $p = 0.001$, two-way ANOVA; D1-saline $p < 0.05$ compared to D1-cocaine and D2-saline, Tukey's post-hoc test; D1/D2 ratio: $U = 1$, $p = 0.02$, Mann-Whitney).

Bar graphs show mean ± SEM. * denotes $p < 0.05$.

Europe PMC Funders Author Manuscripts

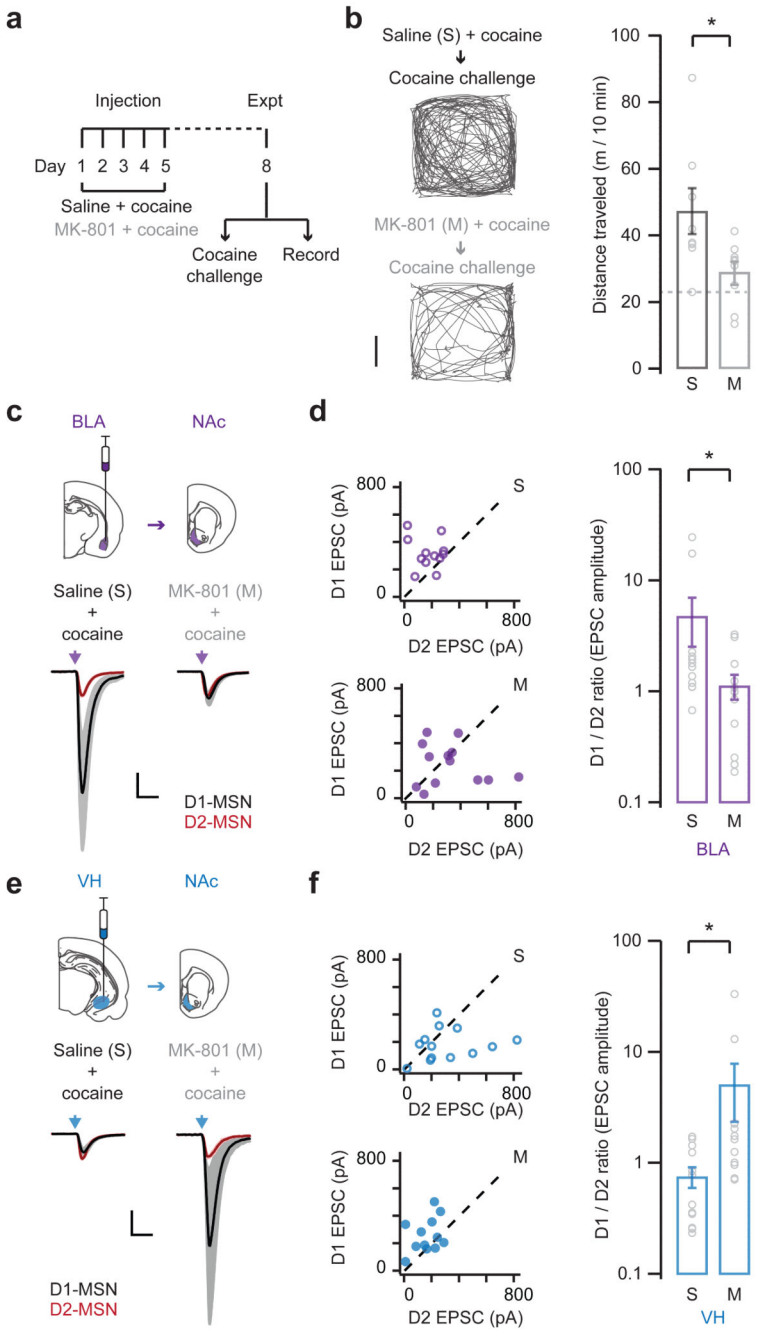

Figure 5. Synaptic reorganization depends on NMDA-Rs

a. Schematic of experimental protocol. Mice were pretreated with MK-801 or saline 30 min before each cocaine injection on days 1 to 5, followed by either a cocaine challenge on day 8 to monitor behavioral sensitization (b), or electrophysiology on day 8 without a cocaine challenge to assess synaptic connectivity (c – f).

b. (Left) Locomotion of saline- (top) or MK-801- (bottom) pretreated mice, measured for 10 min immediately after a cocaine challenge on day 8. Scale bar = 5 cm. (Right) Summary of distance traveled by saline- (s) and MK-801- (m) pretreated mice after the cocaine

challenge. Dashed line indicates saline control. Note that MK-801 abolishes behavioral sensitization (U = 10, p = 0.01, Mann-Whitney; n = 8 (s), 9 (m) mice).

c. (Top) Schematic of AAV-hChR2-mCherry injection in basolateral amygdala (BLA, purple) and projections to the NAc. (Bottom) Light-evoked BLA EPSCs at D1- (black) and D2- (red) MSNs from saline- (left) and MK-801- (right) pretreated mice. BLA EPSCs at D1-MSNs are scaled to neighboring D2-MSNs. Scale bar = unity, 20 ms.

d. (Left) Summary of BLA EPSCs at D1- (top) and D2- (bottom) MSNs in saline- (s) and MK-801- (m) pretreated mice. (Right) Summary of D1/D2 ratio of BLA EPSCs. Note that MK-801 prevents the biasing of BLA EPSCs onto D1-MSNs (D1/D2 ratio: U = 34, p = 0.02, Mann-Whitney; n = 12 (s), 13 (m) pairs).

e, f. Similar to (c, d) for ventral hippocampus inputs (VH). Note that MK-801 also prevents the normalization of VH EPSCs at D1- and D2-MSNs (D1/D2 ratio: U = 25, p = 0.01, Mann-Whitney; n = 13 (s), 11 (m) pairs).

Bar graphs show mean ± SEM. * denotes $p < 0.05$.

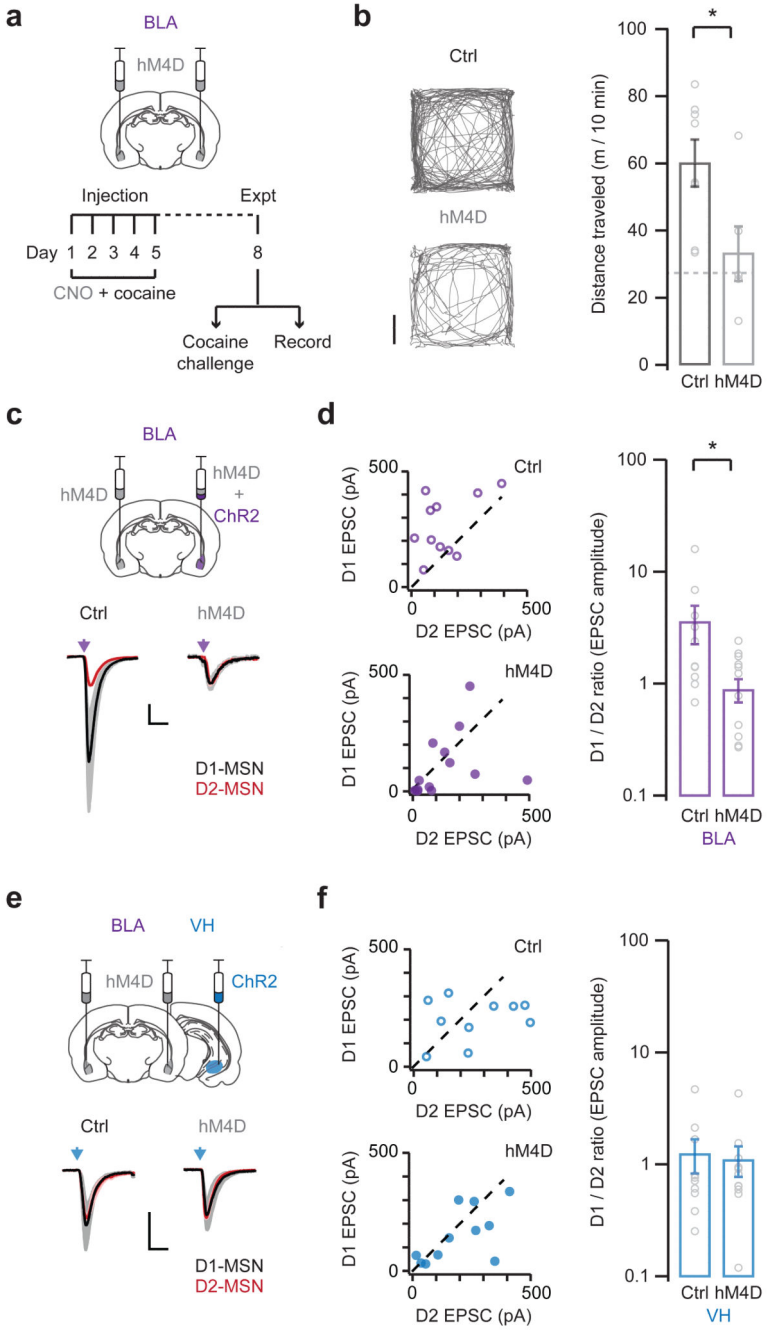

Figure 6. Enhancement of BLA inputs depends on BLA activity

a. Schematic of experimental protocol. (Top) Mice were injected with AAVs to bilaterally express hM4D in the basolateral amygdala (BLA). (Bottom) Two weeks later, mice were pretreated with CNO 30 min before each cocaine injection on days 1 to 5, followed by a cocaine challenge on day 8 to monitor behavioral sensitization (b), or electrophysiology on day 8 without a cocaine challenge to assess synaptic connectivity (c – f).

b. (Left) Locomotion of control (top) or hM4D-expressing (bottom) mice, measured for 10 min immediately after a cocaine challenge on day 8. Scale bar = 5 cm. (Right) Summary of

distance traveled by control or hM4D-expressing mice after the cocaine challenge. Dashed line indicates saline control. Note that inhibiting BLA activity abolishes behavioral sensitization (U = 6, p = 0.02 Mann-Whitney; n = 8 (Ctrl), 6 (hM4D) mice).

c. (Top) Schematic of AAV injection to express hM4D or control GFP bilaterally in the BLA, and ChR2 unilaterally in the BLA. (Bottom) Light-evoked BLA EPSCs at D1- (black) and D2- (red) MSNs from control (left) and hM4D-expressing (right) mice. EPSCs at D1-MSNs are scaled to neighboring D2-MSNs. Scale bar = unity, 20 ms.

d. (Left) Summary of BLA EPSCs at D1- (top) and D2- (bottom) MSNs in control (top) and hM4D-expressing (bottom) mice. (Right) Summary of D1/D2 ratio of BLA EPSCs. Note that inhibiting BLA activity prevents the biasing of BLA EPSCs onto D1-MSNs (D1/D2 ratio: U = 32, p = 0.01, Mann-Whitney; n = 11 (Ctrl), 14 (hM4D) pairs).

e, f. Similar to (c, d), with hM4D or control GFP expressed bilaterally in the BLA, and ChR2 expressed unilaterally in the ventral hippocampus (VH). Note that inhibiting BLA activity does not reverse the normalization of VH EPSCs at D1- and D2-MSNs (D1/D2 ratio: U = 53, p = 0.92, Mann-Whitney; n = 10 (Ctrl), 11 (hM4D) pairs).

Bar graphs show mean ± SEM. * denotes $p < 0.05$.

Europe PMC Funders Author Manuscripts

Europe PMC Funders Author Manuscripts

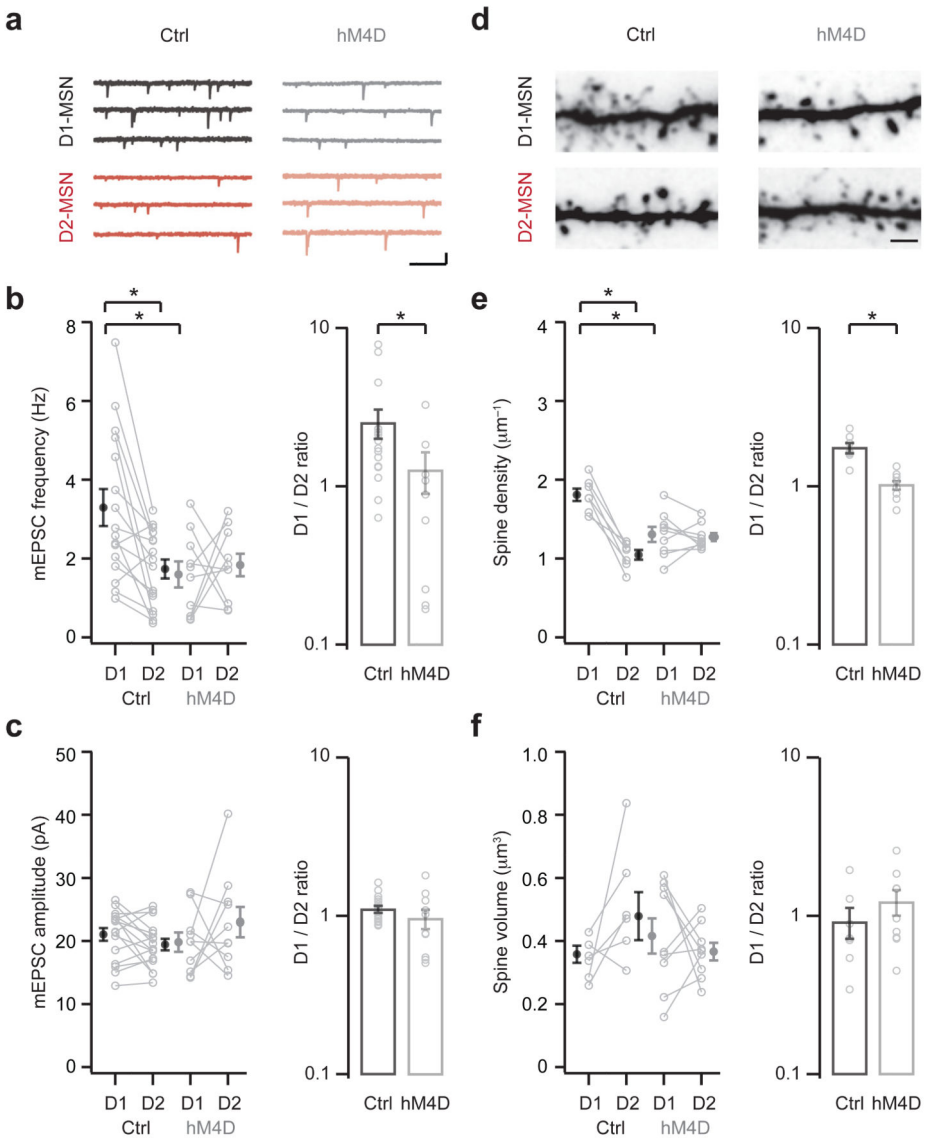

Figure 7. Enhanced connectivity reflects BLA innervation

Mice were injected with AAVs to express hM4D or control GFP bilaterally in the basolateral amygdala (BLA). Two weeks later, mice were pretreated with CNO 30 min before each cocaine injection on days 1 to 5, followed by electrophysiology on day 8 without cocaine challenge.

a. mEPSCs from neighboring D1- (top) and D2- (bottom) MSNs in control (left) or hM4D-expressing (right) mice. Scale bar = 10 pA, 200 ms.

b. Summary of mEPSC frequency at D1- and D2-MSNs in control and hM4D-expressing mice. Note that inhibiting BLA activity blocks the cocaine-induced increase in mEPSC frequency at D1-MSNs (interaction between treatment and cell type, $F_{(1,48)} = 5.7$, p = 0.02, two-way ANOVA; D1-control $p < 0.05$ compared to D1-hM4D and D2-control, Tukey's post-hoc test; D1/D2 ratio: $U = 41$, p = 0.04, Mann-Whitney; n = 16 (Ctrl), 10 (hM4D) pairs).

Europe PMC Funders Author Manuscripts

c. Summary of mEPSC amplitude at D1- and D2-MSNs in control and hM4D-expressing mice. Note no difference in mEPSC amplitude across conditions (no significant effects, two-way ANOVA; D1/D2 ratio: $U = 58$, $p = 0.26$, Mann-Whitney).

d. Two-photon images of dendrites and spines at neighboring D1- (top) and D2- (bottom) MSNs in control (left) or hM4D-expressing (right) mice. Scale bar = 2 μm.

e. Summary of spine density at D1- and D2-MSNs in control and hM4D-expressing mice. Note that inhibiting BLA activity blocks the cocaine-induced increase in spine density at D1-MSNs (interaction between treatment and cell type, $F_{(1,28)} = 23.4$, $p < 0.001$, two-way ANOVA; D1-control $p < 0.05$ compared to D1-hM4D and D2-control, Tukey's post-hoc test; D1/D2 ratio: $U = 1$, $p < 0.001$, Mann-Whitney; n = 7 (Ctrl), 9 (hM4D) pairs).

f. Summary of spine volume at D1- and D2-MSNs in control and hM4D-expressing mice. Note no difference in spine volume across conditions (no significant effects, two-way ANOVA; D1/D2 ratio: $U = 21$, $p = 0.3$, Mann-Whitney).

Bar graphs show mean ± SEM. * denotes $p < 0.05$.